Journal of Theoretical Biology 509 (2021) 110498

Contents lists available at ScienceDirect

Journal of Theoretical Biology

journal homepage: www.elsevier.com/locate/yjtbi

Density dependent Resource Budget Model for alternate bearing

Shadisadat Esmaeili [a,*], Alan Hastings [a,d], Karen Abbott [b], Jonathan Machta [c,d], Vahini Reddy Nareddy [c]

[a] Department of Environmental Science and Policy, One Shields Avenue, University of California, Davis, CA 95616, USA
[b] Department of Biology, Case Western Reserve University, 10900 Euclid Ave, Cleveland, OH 44106, USA
[c] Physics Department, University of Massachusetts, Amherst, MA 01003, USA
[d] Santa Fe Institute, 1399 Hyde Park Road, Santa Fe, NM 87501, USA

ARTICLE INFO

Article history:
Received 21 April 2020
Revised 14 September 2020
Accepted 15 September 2020
Available online 21 September 2020

Keywords:
Masting
Biennial bearing
Variable fruit production
Synchrony

ABSTRACT

Alternate bearing, seen in many types of plants, is the variable yield with a strongly biennial pattern. In this paper, we introduce a new model for alternate bearing behavior. Similar to the well-known Resource Budget Model, our model is based on the balance between photosynthesis or other limiting resource accumulation and reproduction processes. We consider two novel features with our model, 1) the existence of a finite capacity in the tree's resource reservoir and 2) the possibility of having low (but non-zero) yield when the tree's resource level is low. We achieve the former using a density dependent resource accumulation function, and the latter by removing the concept of the well-defined threshold used in the Resource Budget Model. At the level of an individual tree, our model has a stable two-cycle solution, which is suitable to model plants in which the alternate bearing behavior is pronounced. We incorporate environmental stochasticity by adding two uncorrelated noise terms to the parameters of the model associated with the nutrient accumulation and reproduction processes. Furthermore, we examine the model's behavior on a system of two coupled trees with direct coupling. Unlike the coupled Resource Budget Model, for which the only stable solution is the out-of-phase solution, our model with direct coupling has stable in-phase period-2 solutions. This suggests that our model might serve to explain spatial synchrony on a larger scale.

1. Introduction

"Alternate bearing" is the variability of fruit or nut production in many types of plants for which a year of high yield (ON-year) is followed by one or more years of low or no production (OFF-years). Generally, the crop varies biennially. However, in some cases, it can show longer period cycles where multiple years of high or low yield happen consecutively (Monselise and Goldschmidt, 1982; Shalom et al., 2012). When this phenomenon is observed in collective synchrony among trees in orchards and natural forests, it is known as masting.

Alternation is very common and is observed in a variety of plants like citrus trees (Shalom et al., 2012), olive trees (Lavee, 2007), and pistachio trees (Lyles et al., 2015; Noble et al., 2018). These plants are different in many ways. The differences include time of flowering, dormancy, and duration of fruiting compared to vegetative growth (Monselise and Goldschmidt, 1982). The ubiquity of the phenomenon suggests that there is a common mechanism that explains the crop variability in a variety of plants.

Both exogenous conditions, like environmental triggers, and endogenous factors, like bud abscission, flowering inhibition by current fruits (Shalom et al., 2012), pollination, and fruit overload, have been considered as contributing factors to the alternate bearing phenomenon. The depletion of the resource level of the plant due to over-fruiting is considered the most common cause of the phenomenon (Monselise and Goldschmidt, 1982; Lavee, 2007). Isagi pioneered a simple model to explain the mechanism of variable acorn yield observed at the level of an individual tree (Isagi et al., 1997). His model, called the Resource Budget Model (RBM), is based on the dynamics of the tree's energy resource which is accumulated as the result of photosynthesis and consumed during the flowering and nut production processes.

The Resource Budget Model, as originally proposed by Isagi et al. (1997) and expanded in Satake and Iwasa (2000), assumes the existence of a well-defined threshold for the tree's resource levels below which the plant will not reproduce. This means that during an OFF-year, the tree has no yield. This assumption is appropriate for the plants like olive and citrus, for which there is zero or

* Corresponding author.
E-mail addresses: sesmaeili@ucdavis.edu (S. Esmaeili), amhastings@ucdavis.edu (A. Hastings), kca27@case.edu (K. Abbott), machta@umass.edu (J. Machta), vnareddy@umass.edu (V.R. Nareddy).

https://doi.org/10.1016/j.jtbi.2020.110498
0022-5193/

near-zero yield during an OFF-year, but represents other species with low but positive OFF-year yields less well. Once the resource level of the tree exceeds the threshold, flowering and nut production happens. Both flowering and nut production processes are costly and result in the depletion of the tree's resource reservoir. The cost of flowering and nut production is assumed to be proportional to the amount of resources above the threshold with the depletion coefficient (the parameter of the model). The Resource Budget Model belongs to the category of tent maps for which there is no stable period-2 solution at the level of individual tree (except at the bifurcation point). Systems of two trees do have an in-phase period-2 solution, but it is only stable if the trees are coupled via indirect (mean-field) coupling, as with pollination, and not for trees coupled directly through local interactions like root grafting (Prasad et al., 2017). Together, these features make the Resource Budget Model a simple and successful model to explain the masting phenomenon in many plants for which there is zero or near-zero yield during an OFF-year, the plant goes through several OFF-years before having a year with high yield, and at a collective level, the plants can interact via pollination (the plants are monoecious). But the model needs to be modified if it is to be applied to the plants like pistachio that have a low yield, but not zero, during OFF-years, whose yield show a two-cycle behavior, and is dioecious, therefore, the interaction between the female trees happens via direct coupling (root grafting). Lyles et al. modified the Resource Budget Model by removing the concept of threshold from the model and adding temporal stochasticity to the depletion coefficient and the pollen availability to achieve the variable and synchronized nut production of the trees (Lyles et al., 2015). However, this model, like the previous Resource Budget Models, does not show synchrony in trees with direct coupling.

In another attempt to predict the yield of citrus trees, Ye and Sakai suggested a more generalized version of the Resource Budget Model (Ye and Sakai, 2016). Motivated by the result of their analysis of field data collected from a citrus orchard in Japan (Ye et al., 2008), they added a vegetative growth factor to the Resource Budget Model to account for the role of new leaf growth in inhibition of fruit production. According to their model, the cost of new leaf growth is proportional to the empty portion of the resource tank. Also, the return map obtained from their experimental study showed, what they called, a "hump-shaped" curve similar to what is obtained from the logistic map. To reproduce the logistic-like return map, they replaced the linear relationship between the resource reserve level and flowering and fruiting cost in the original Resource Budget Model (see Section 2), with a nonlinear Ricker-type relationship (Ye and Sakai, 2016). By adding nonlinearity they modified the model to better reflect the yield dynamics of citrus trees. However, similar to the original Resource Budget Model, this model assumes the existence of a well-defined threshold below which no flowering or production happens, which does not reflect the low (but non-vanishing) yield of species, like pistachio, during OFF years.

Inspired by an existing data set collected from a pistachio orchard at the level of individual trees during a 6-year period (Lyles et al., 2015; Noble et al., 2018), we propose a different approach for modeling alternate bearing that accommodates low but non-vanishing yield during OFF-years. This is achieved by replacing the concept of a sharp cut-off for reproduction (represented by a threshold function) with a continuous function that accommodates the non-zero yield when the tree's current energy level is low. Also, we take into account the fact that there is a maximum capacity for the plant to store photosynthate and other nutrients and therefore, its energy storage cannot grow indefinitely.

In Section 2 we briefly review the rules and the characteristics of the Resource Budget Model. In Section 3, we describe our new model of alternate bearing behavior for the trees with low yield during OFF-years. We analyze the model by performing a bifurcation analysis. Furthermore, we discuss and apply some necessary constraints on the model to make it biologically meaningful and applicable. In Section 4, we add stochasticity to the model to account for environmental variation. As the preliminary step to understand the collective behavior of the trees in an orchard or a natural forest, in Section 5, we study the dynamics of a two-tree system.

2. Background

First we describe the Resource Budget Model: every year, the resource level of an individual tree (S_t) increases by a constant amount called P_s. If the resource level exceeds a threshold, L_T, the plant will flower and bear fruits/nuts which depletes the energy reservoir of the tree. The cost of flowering is assumed to be proportional to the excess amount of resources above the threshold with a positive constant a. The cost of fruit/nut production is also considered to be proportional to the cost of flowering. The Resource Budget Model is formulated as,

$$S_{t+1} = \begin{cases} S_t + P_s, & S_t + P_s \leqslant L_T \\ S_t + P_s - a\,(R_c + 1)\,(S_t + P_s - L_T), & S_t + P_s > L_T \end{cases} \quad (1)$$

where R_c is the ratio of the cost of fruit/nut production to the cost of flowering. The model can be written in terms of the dimensionless variable $s_t = \frac{S_t + P_s - L_T}{P_s}$ as,

$$s_{t+1} = \begin{cases} s_t + 1, & s_t \leqslant 0 \\ -m s_t + 1, & s_t > 0 \end{cases} \quad (2)$$

where $m = a(R_c + 1) - 1$ is called the depletion coefficient.

As it is shown in the model's orbit diagram (Fig. 1) and discussed in Appendix A, the model has a stable fixed point for $m < 1$. At exactly $m = 1$ (which is the discontinuous bifurcation point) the system shows two-cycle behavior. For $m > 1$ the system demonstrates a chaotic period-four oscillation for a very small range of the parameter, followed by a single band chaos (Prasad and Sakai, 2015).

3. The Model

Similar to the Resource Budget Model, our new model of alternate bearing is based on the dynamics of the nutrient (i.e. carbon, nitrogen, phosphorus, etc) level of an individual tree. According to our model, the nutrient level of an individual tree in year $t + 1$ is determined based on the balance between two processes that happen in year t: 1) nutrient accumulation, 2) reproduction. The accumulation of nutrients is the result of photosynthesis (Marino et al., 2018) and the plant's interaction with soil and soil-based microorganisms (Guignard et al., 2017). The process of reproduction is the flowering and production of nuts. Nut production comes with a higher cost than flowering and is considered the main sink of the tree's nutrient reservoir (Marino et al., 2018). The nutrient level of a tree in year $t + 1$ (S_{t+1}) can be written as,

$$S_{t+1} = S_t + \text{Nutrient Accumulation} - \text{Cost of Reproduction}. \quad (3)$$

In modeling the Nutrient Accumulation and the Cost of Reproduction, we take into account the following considerations:

1) The Nutrient Accumulation process cannot result in the indefinite growth of the tree's nutrients level. In other words, each tree has a maximum capacity to store nutrients, denoted by S_{max}. Therefore, the amount of nutrients that is added to the tree's reservoir each year is a density dependent function of its existing nutrients level. We model the Nutrient Accumulation process by a function of S_t, which grows when S_t is small but approaches zero as $S_t \to S_{max}$.

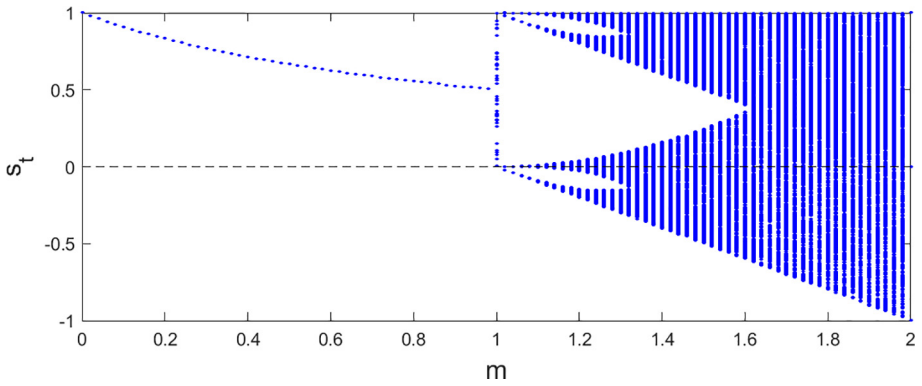

Fig. 1. The orbit diagram of the Resource Budget Model shows that the dynamics of the system goes from a stable fixed point for the depletion coefficient, $m < 1$, to period-four oscillation for a very small range of m and then quickly leading to chaos.

2) As we mentioned in the introduction, the function used to model the Cost of Reproduction should allow for low yield (as opposed to zero yield) during OFF-years.

There are many mathematical functions that satisfy the above conditions and can be considered to model these two processes. For the purpose of this paper, we have chosen the bounded growth function for Nutrient Accumulation and a shifted sigmoid function for the Cost of Reproduction. However, these functions are not unique. In Appendix C, we present an alternate version of the model using a different Nutrient Accumulation function and show that the dynamics of the model stay qualitatively similar.

Bounded Growth Function

The amount of nutrients added to the tree's reservoir as a result of photosynthesis and other nutrient uptake processes at the end of year t is modeled by:

$$\text{Nutrient Accumulation} = S_{max}(1 - e^{-r_1 S_t/S_{max}}) - S_t, \tag{4}$$

where S_t is the current nutrients level, S_{max} is the tree's maximum capacity to store nutrients, and r_1 is the efficiency of the Nutrient Accumulation process. Fig. 2a shows the behavior of the nondimensionalized version of Eq. (4) as a function of $s_t = \frac{S_t}{S_{max}}$ and for different values of r_1. As r_1 gets larger, the tree can accumulate more nutrients and do it more efficiently and with less available resources. Therefore the accumulation function has a higher maximum and is right skewed with increasing r_1 (the accumulation function reaches its maximum for a smaller current resource levels (s_t)).

Shifted Sigmoid Function

The cost of reproduction is modeled by a vertically shifted sigmoid function. A sigmoid function allows for low production when the current nutrients level is low. Also, the second term (vertical shift) ensures that when $S_t = 0$, there is no reproduction, and therefore no cost.

$$\text{Cost of Reproduction} = \frac{S_{max}}{1 + e^{(-r_2 S_t + L)/S_{max}}} - \frac{S_{max}}{1 + e^{L/S_{max}}}. \tag{5}$$

In Eq. (5), r_2 is the tree's reproductive investment and L/r_2 ($=L^*$) is the threshold that controls the level of resource needed to trigger high yield. We can nondimensionalize Eq. (5) by defining $s_t = \frac{S_t}{S_{max}}$ and $l = \frac{L}{S_{max}}$. Fig. 2b and c show the behavior of the nondimensionalized versions of the Cost of Reproduction for different values of the efficiency rate (r_2) and the threshold (l).

As it can be seen in Fig. 2a, there are values of r_1 for which the Nutrient Accumulation term becomes negative. Also, for some values of r_2 and l, the curves in Fig. 2b and c cross the diagonal line which indicates that the Cost of Reproduction exceeds the current resource levels (s_t). For the model to be meaningful, both of these conditions must be avoided. This can be done by imposing constraints on the model and defining acceptable ranges of parameters. Section 3.2 addresses this issue in detail.

Finally, we can write the nondimensionalized model as,

$$s_{t+1} = (1 - e^{-r_1 s_t}) - \left(\frac{1}{1 + e^{(-r_2 s_t + l)}} - \frac{1}{1 + e^{l}}\right). \tag{6}$$

While Eq. (6) models the dynamics of a tree's nutrients level, the amount of nut production is the observable that is actually measured for each tree. Since nut production is the main sink of the tree's nutrient resources during reproduction, it can be taken to be proportional to the cost of reproduction. We use $Y_t = \frac{1}{1+e^{(-r_2 s_t + l)}} - \frac{1}{1+e^{l}}$ to denote the nondimensionalized yield of a tree at time t to also study the dynamics of the observable of the system.

3.1. Bifurcation analysis

In this section we study the behavior of the model for different values of efficiency rates and a fixed value of l. For simplicity, we choose the accumulation efficiency and reproductive investment rates (r_1 and r_2) to always be equal. Therefore, we will have $r_1 = r_2 = r$. This will simplify the model to a one-dimensional, single parameter map, many examples of which have been extensively explored (Strogatz, 1994; Devaney, 2003; Feigenbaum, 1980). However, the results presented in this section remain qualitatively the same if r_1 and r_2 are chosen to be different.

Fig. 3a and b show the orbit diagram of the model and the tree's yield (Y_t) respectively, when $l = 7$. Qualitatively, the orbit diagrams are similar to orbit diagrams of one dimensional unimodal maps with one parameter, like the quadratic map. The model has a stable fixed point for $r \lesssim 6.8$. At $r \approx 6.8$ the first period-doubling bifurcation happens. For $6.85 \lesssim r \lesssim 8.6$ the model shows a 2-cycle behavior (the range of the parameter where the alternate bearing behavior can be modeled). At $r \approx 8.6$ a second period-doubling bifurcation happens and the system switches to a 4-cycle oscillation. Next period-doubling bifurcation happens at $r \approx 9.1$ followed by a cascade of period-doubling bifurcations that leads to chaos. Like the orbit diagrams of other unimodal maps, the chaotic regime is interrupted by small windows of cyclic behavior. Fig. 3c shows the Lyaponov exponent as a function of the parameter r. We used the method introduced in (Strogatz, 1994) to calculate the Lyaponov exponent. For the range of the parameter values where $\lambda < 0$ the system has a stable fixed point or a cyclic attractor. When $\lambda \to -\infty$, the attractor is superstable. Period-doubling bifurcations happen when $\lambda = 0$. For $\lambda > 0$ the trajectories diverge exponentially which is a signature of a chaotic regime.

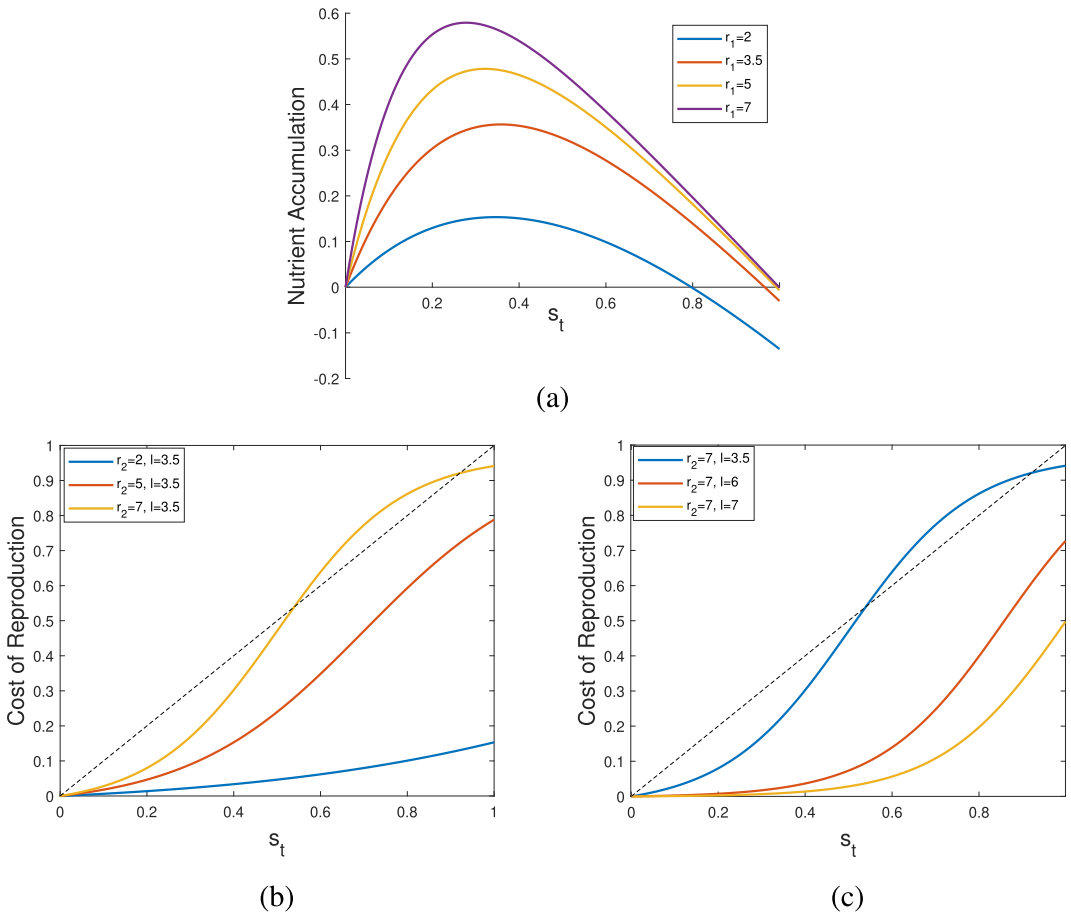

Fig. 2. The behavior of a) nondimensionalized Nutrient Accumulation term for different values of r_1, b) and c) nondimensionalized Cost of Reproduction for different values of r_2 when $l = 3.5$, and different values of l when $r_2 = 7$, respectively.

Fig. 4 shows the trajectories for different values of r belonging to different regimes, again with $l = 7$. For $r = 6$, the model relaxes to a stable fixed point (Fig. 4a) and the tree maintains a fixed carbon level and constant yield. For $r = 7.5$, the carbon level, and therefore the production, show a period-2 oscillation (Fig. 4b). Fig. 4c shows the model's stable period-4 solution for $r = 8.8$. When $r = 9.8$ the system is in the chaotic regime (Fig. 4d).

The analysis in this section has also been performed for different values of l. As we change l, the locations of the period-doubling bifurcations and the width of the chaotic windows change, but the behavior of the model stays qualitatively the same.

3.2. Constraints on the Model

As we briefly mentioned in Section 3, for a range of values of r_1, the Nutrient Accumulation term becomes negative. Also, for some combinations of r_2 and l the Cost of Reproduction exceeds the current resource levels (s_t). To avoid this and for the model to be biologically meaningful, we have to determine the acceptable range of values for the model's parameters.

3.2.1. Nutrient Accumulation

The Nutrient Accumulation process should always result in the increase of current resource levels. This means that the result of Eq. (4) should always be greater than zero when the current resource levels are below the maximum capacity (i.e. $S_t < S_{max}$ or $s_t < 1$). As $S_t \to S_{max}$ ($s_t \to 1$), the Nutrient Accumulation function should approach zero. In other words, $S_t = S_{max}$ ($s_t = 1$) should be the stable fixed point of the model when the reproduction is turned off. This means that the solution of Eq. (7) (Nutrient Accumulation $= 0$) should be $s^* = 1$.

$$1 - e^{-r_1 s^*} - s^* = 0. \tag{7}$$

In Fig. 2a, s^* is where each curve crosses the horizontal axis. As we can see, for any finite values of r_1, the solution to the Eq. (7) is less than 1. This means for $s^* < s_t \leq 1$ the result of the Nutrient Accumulation function is negative. As it can be seen in Fig. 2a, as r_1 becomes larger, s^* gets closer to 1 and the result of the Nutrient Accumulation function remains positive for a larger range of s_t. Our goal is to find a lower bound for r_1 (let's call it r_{min}) so that for values of r_1 greater than r_{min} the corresponding s^* is sufficiently close to 1. We can write $s^* = 1 - \delta$, where δ is the tolerance that controls the proximity of s^* to 1. To determine the r_{min} as a function of δ, in Eq. (7), we substitute r_1 with r_{min} and s^* with $1 - \delta$. we can write,

$$1 - e^{-r_{min}(1-\delta)} - (1 - \delta) = 0. \tag{8}$$

Solving for r_{min}, we obtain a lower bound for r_1 as a function of δ (i.e. $r_1 \geqslant r_{min}(\delta)$), where $r_{min}(\delta) = \frac{1}{1-\delta} \ln\left(\frac{1}{\delta}\right)$. For any value of r_1 greater than r_{min} we can accept that the Nutrient Accumulation term remains positive for $s_t \in (0, 1 - \delta) \approx (0, 1)$. For the rest of this manuscript, we choose $\delta = 0.01$ and study the behavior of the model for $r_1 \geqslant 4.65$.

3.2.2. Cost of Reproduction

A tree's intensity of flowering and nut production depends on the current level of its nutrients storage. A tree will never draw more resource to flower and reproduce than what is available in

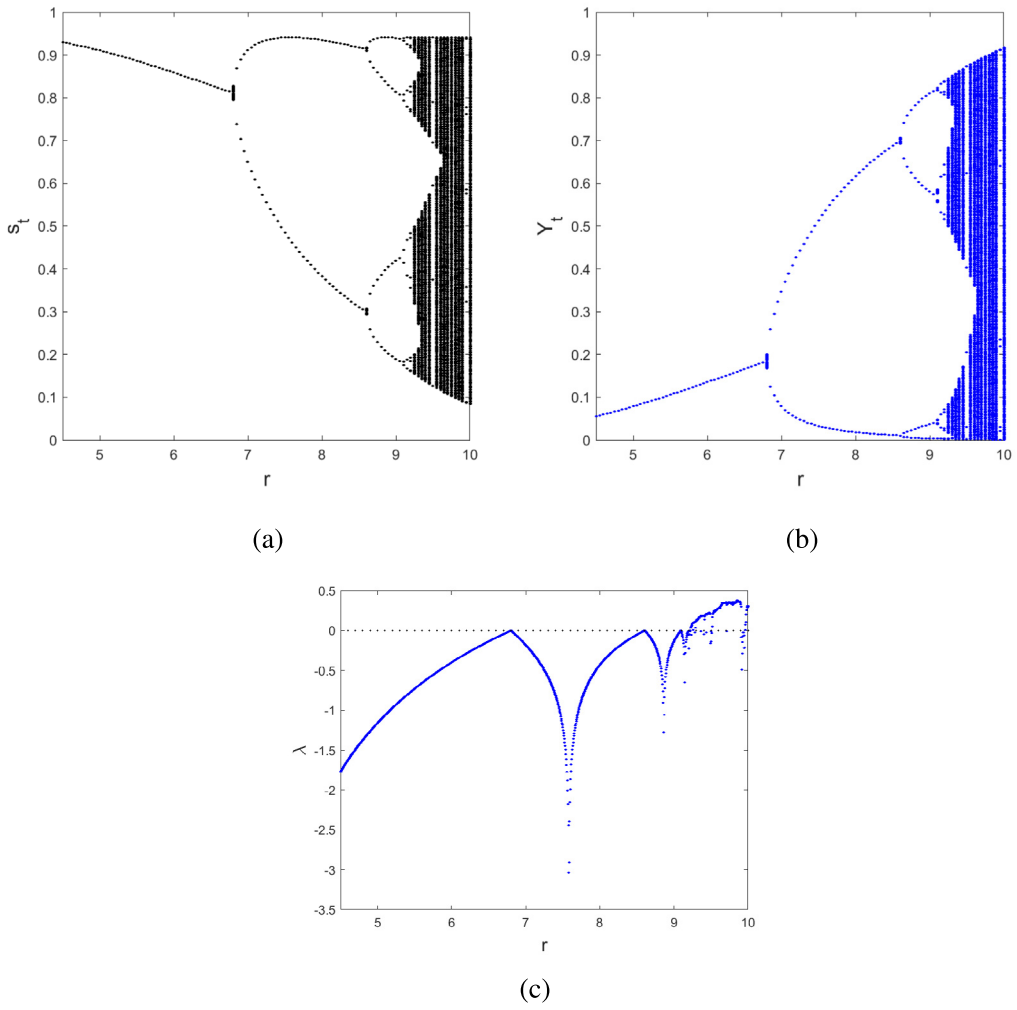

Fig. 3. a) The orbit diagram of the model for $r_1 = r_2 = r$ and $l = 7$, b) the orbit diagram of the tree's yield Y_t, and c) the corresponding Lyaponov exponent (λ) as a function of r. For values of r where $\lambda > 0$ the system is in the chaotic regime.

its reservoir. In the language of our model, the Cost of Reproduction (Eq. (5)) cannot exceed the current nutrient levels. In terms of the density of nutrient levels, s_t, it means:

$$\left(\frac{1}{1+e^{(-r_2 s_t + l)}} - \frac{1}{1+e^{l}}\right) \leqslant s_t. \tag{9}$$

As presented in Fig. 2b and c, for some combinations of r_2 and l, the above condition is not met. To find the acceptable (r_2, l) pairs, for which the condition is satisfied, we solved Eq. (9) numerically. The shaded area in Fig. 5 shows the acceptable pairs of (r_2, l) for which the cost of reproduction does not exceed the current nutrient levels.

4. The role of environmental variation

The stochastic effect of environmental variation plays an important role in photosynthesis (and other nutrient uptake processes) and reproduction. Factors like the amount of CO_2, the intensity of radiant energy, and the temperature affect the process of photosynthesis (Marshall and Biscoe, 1980). On the other hand, the amount of precipitation and the temperature during the reproduction season affect flowering or nut production. We incorporate environmental variability into the model by adding two noise terms to the nutrient accumulation efficiency and reproductive investment rates (r_1 and r_2 respectively),

$$s_{t+1} = 1 - e^{-(r_1+\xi_{1t})s_t} - \left(\frac{1}{1+e^{(-(r_2+\xi_{2t})s_t + l)}} - \frac{1}{1+e^{l}}\right) \tag{10}$$

in which ξ_{1t} and ξ_{2t} are uncorrelated random variables that are independently drawn from a normal distribution with mean zero and variances σ_1^2 and σ_2^2, respectively.

In our simulations we choose $r_1 = r_2 = r = 7$ and $l = 7$ for which the system is in the two-cycle regime. We also set $\sigma_1 = \sigma_2 = \sigma$. Notice that these choices of parameters satisfy the conditions set for r_1, r_2, and l as mentioned in Section 3.2 and shown in Fig. 5. While under the effect of very large noise, these conditions can be violated, for the small enough variance of the noise terms, our choices of parameters are unlikely to go beyond the acceptable range. Fig. 6a shows a perfect period-two behavior of the model without noise. Fig. 6b–d show the effects of noise with different strengths (variances, σ) on the amplitude and the phase of the oscillation.

5. The dynamics of a two-tree system

One of the mechanisms behind spatial synchrony, observed in the masting phenomenon, is the local interaction between trees.

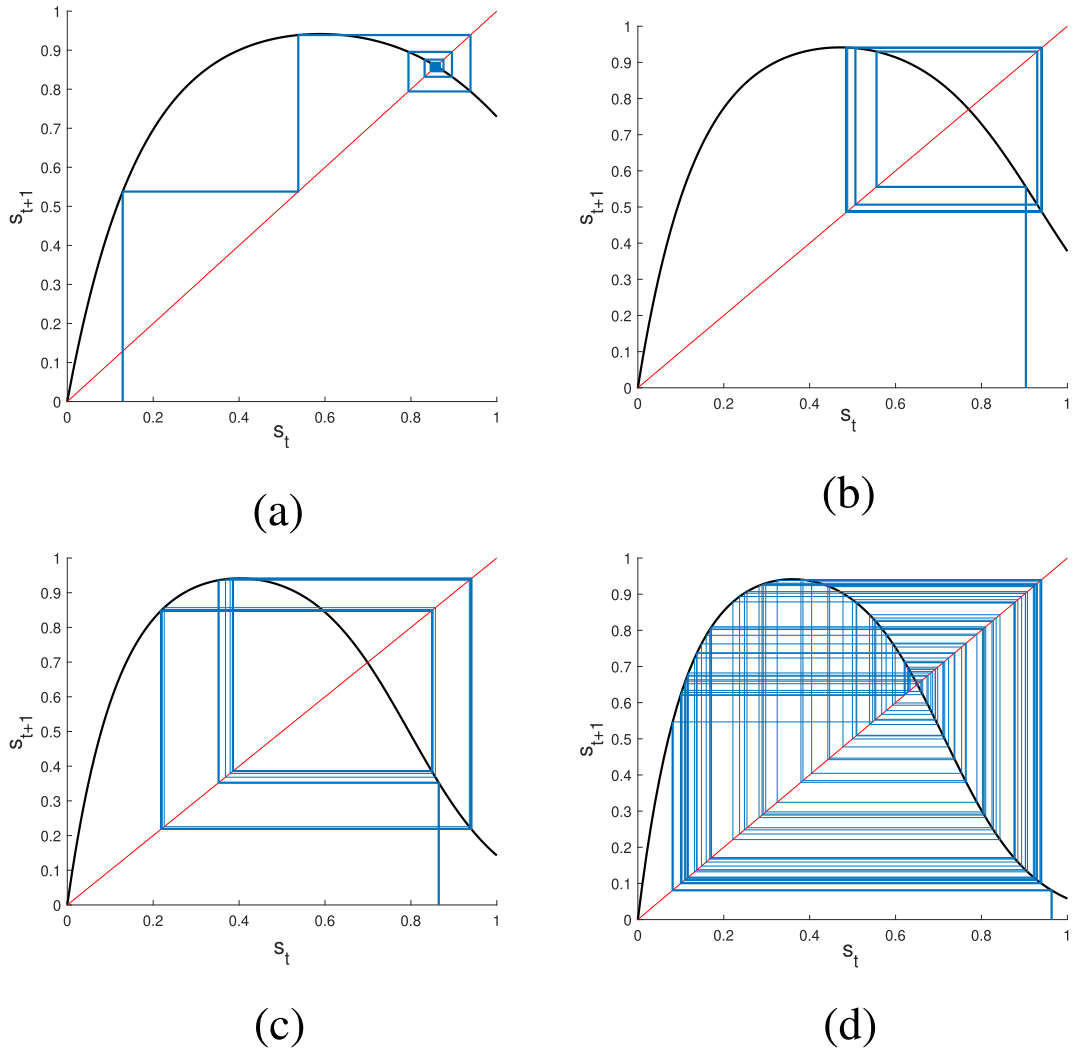

Fig. 4. The trajectories for different values of r. a) $r = 6$, the model relaxes to a stable fixed point, b) $r = 7.5$, it shows a stable period-two oscillation, c) $r = 8.8$, the model has a period-four solution, d) $r = 9.8$, the systems is in the chaotic regime. In all panels $l = 7$.

The trees planted in proximity to one another interact in complex ways including exchanging their carbon through root grafts (Klein et al., 2016). Grafting is known as direct interaction or diffusive coupling (Prasad et al., 2017). Trees also interact through pollination via external agents (e.g. birds, insects, and wind). This process is considered an indirect interaction and usually implemented in the form of mean-field coupling (Satake and Iwasa, 2000; Prasad et al., 2017). In dioecious plants, pollen distribution is provided by male trees while flowering and reproduction are done by female trees. Therefore, pollination cannot be considered as the mechanism behind the interaction among female trees. Instead, root grafting (direct coupling) should be considered as the method of local interaction. The numerical simulations of the Resource Budget Model with direct coupling for a system of two trees show that the only possible period-2 solution for the trees is the out-of-phase solution (Prasad et al., 2017). We confirmed these results by performing a stability analysis of the coupled Resource Budget Model as discussed in Appendix B. These results suggest that the Resource Budget Model cannot model the spatial synchrony observed among dioecious plants, like pistachios, for which the direct coupling is the main method of interaction.

In this section we use direct coupling to investigate the dynamics of a deterministic system of two coupled trees. The internal

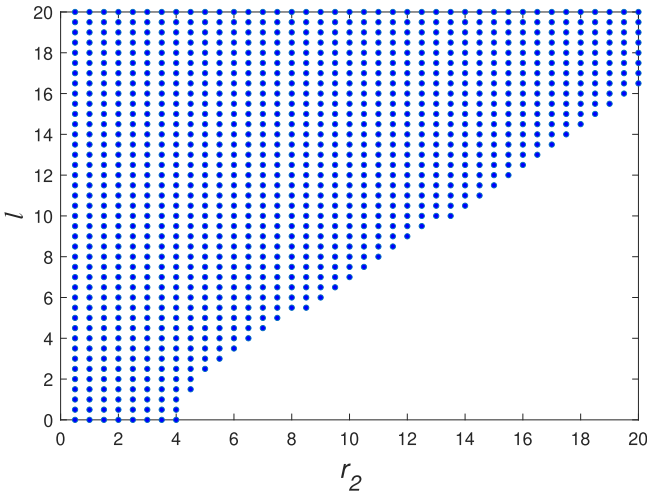

Fig. 5. The area covered by blue dots shows the combinations of (r_2, l) for which the condition in Eq. (9) is satisfied and the Cost of Reproduction stays below the current nutrient levels.

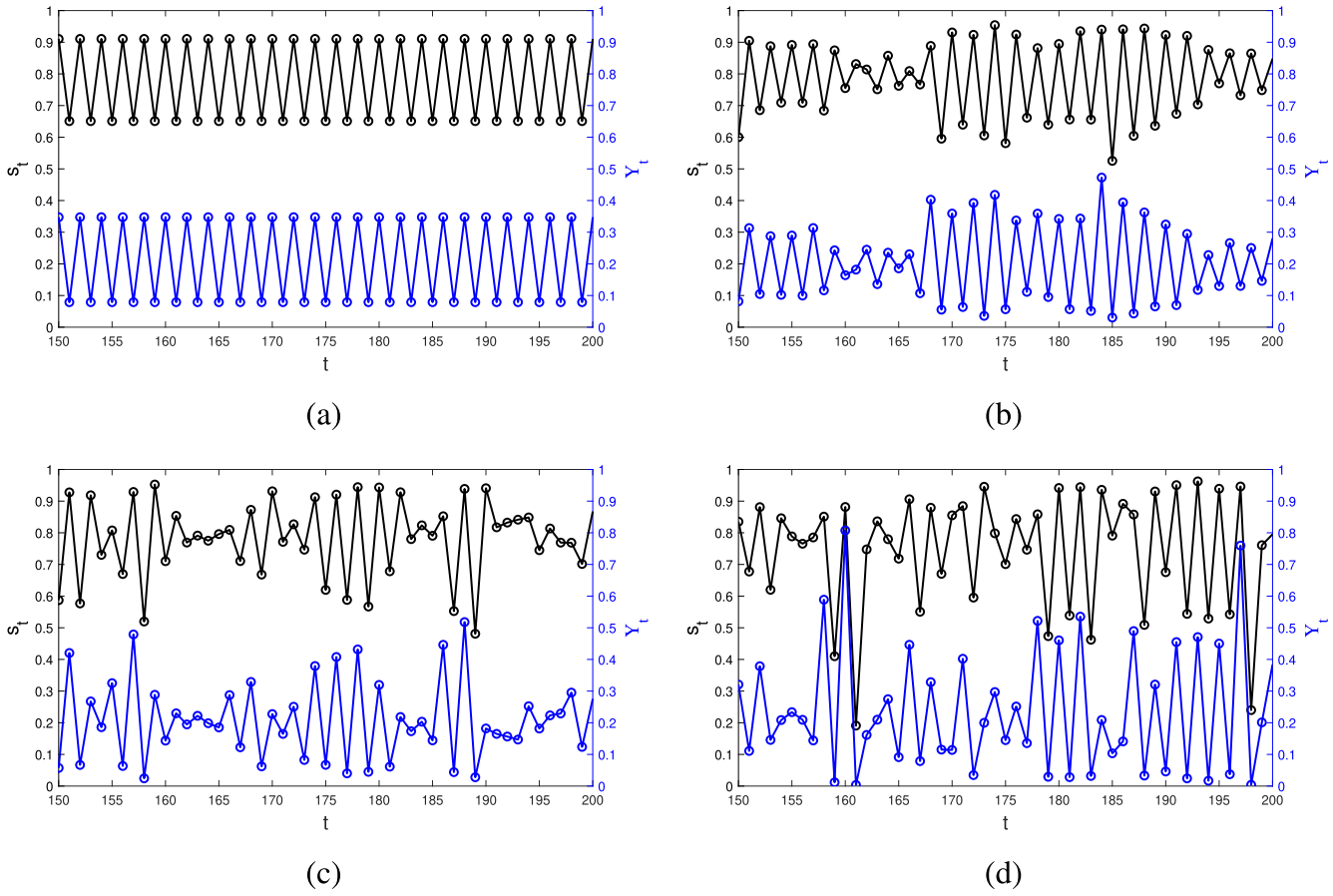

Fig. 6. The behavior of the density of resources (black) and the yield (blue) for 50 years for $r = 7,\ l = 7$, and a) $\sigma = 0$ (no noise), b) $\sigma = 0.25$, c) $\sigma = 0.5$, and d) $\sigma = 0.75$. (For interpretation of the references to color in this figure legend, the reader is referred to the web version of this article.)

dynamics of each tree is defined by Eq. (6). We use $\tilde{s}_{i,t}$ $(i = 1, 2)$ to refer to each tree's resource level after nutrient uptake and reproduction but before exchange of resources. Each tree shares a fixed fraction of its resource (κ) with its neighboring tree and receives the same fraction of the second tree's resource in return. The result is a net flow of nutrient from one tree to another. The nutrient level of each tree at the beginning of year $t + 1$ is:

$$\begin{aligned} s_{1,t+1} &= \tilde{s}_{1,t} + \kappa(\tilde{s}_{2,t} - \tilde{s}_{1,t}) \\ s_{2,t+1} &= \tilde{s}_{2,t} + \kappa(\tilde{s}_{1,t} - \tilde{s}_{2,t}). \end{aligned} \tag{11}$$

To understand the dynamics of this system, we solve Eqs. (11) numerically to construct the orbit diagram. We assume both trees have the same internal dynamics by choosing the same nutrient accumulation efficiency and reproductive investment rates. Also, similar to previous sections we simplify the model by setting the nutrient accumulation efficiency and reproductive investment rates to be equal. Therefore, the internal dynamics of both trees only depend on one parameter, r. We also choose $l = 7$ for both trees. To build the orbit diagram, we follow the technique used in (Hastings, 1993). We choose 20 random initial conditions for each choice of parameters r and κ to capture all stable solutions where the system is multistable.

Fig. 7 shows the dependence of the system's dynamics on parameter r and different values of κ. Similar to the coupled logistic equations discussed in (Hastings, 1993), two general categories of solutions are identified: the perfectly in-phase solutions where $s_{1,t} = s_{2,t}$ and all the other solutions, which we refer to as out-of-phase solutions, where $s_{1,t} \neq s_{2,t}$. The left column in Fig. 7 shows the orbit diagram of the total nutrient levels $(s_{1,t} + s_{2,t})$ for stable in-phase solutions. The right column shows the orbit diagram of the nutrient levels difference $(s_{1,t} - s_{2,t})$ when the system has a stable out-of-phase solution. For the range of parameters for which the in-phase and out-of-phase solution coexist, both solutions are shown in red. Different patterns of oscillation are observed in both in-phase and out-of-phase categories. These patterns include in-phase or out-of-phase period-2, period-3, period-4, or higher period oscillations, as well as chaotic behavior. When the resource exchange between the two trees is weak (e.g. $\kappa = 0.05$), as shown in Fig. 7a and b, the out-of-phase solutions are more prevalent and the in-phase solutions are mostly observed when the two trees are in fixed point or oscillatory regimes with different periods. As the interaction becomes stronger, the in-phase solutions appear for a wider range of parameter r and chaotic in-phase solutions are more commonly observed. For a strong enough κ (e.g. $\kappa = 0.2$) the trees predominantly stay in-phase while out-of-phase solutions are observed for $r \geqslant 9.7$. The similarity between Figs. 7c and 3a suggests that, in this case, the system behaves mostly like a single unit system.

As we mentioned above, the category of in-phase solutions include a variety of periodic and chaotic oscillations that emerge for different values of parameter r. Fig. 8 compares the basin of attraction of some of these solutions. To obtain Fig. 8c–f, we scan the entire phase space of $(s_{1,0}, s_{2,0})$, with increment of 0.005, to find the initial conditions that relax to an in-phase attractor for $\kappa = 0.1$ and a given value of r. Fig. 8c–j are color coded to match the marker lines in Fig. 8a and b. We choose values of r for which the in-phase and out-of-phase solutions coexist. The in-phase solutions studied

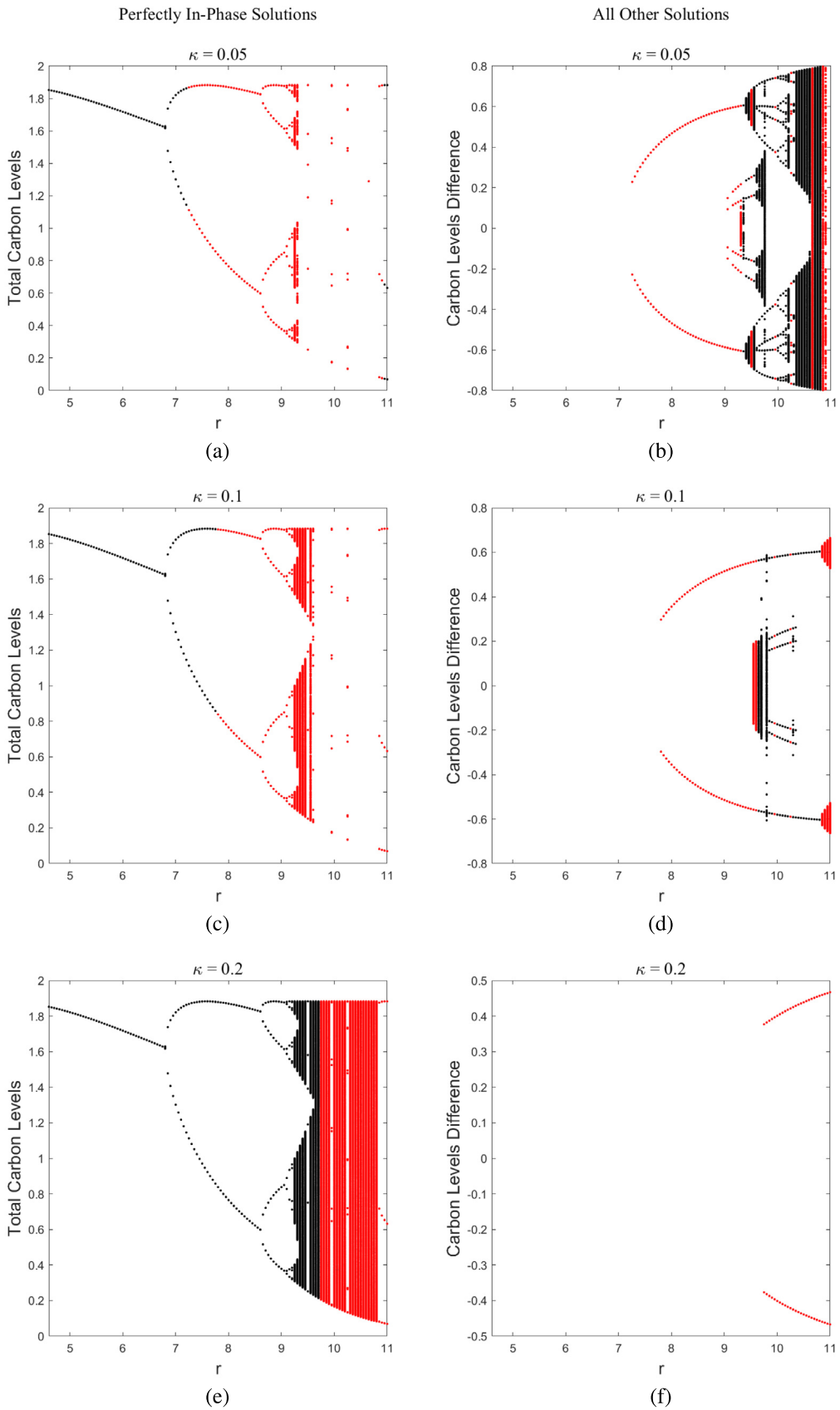

Fig. 7. Left column: orbit diagrams of the total carbon levels when $s_{1,t} = s_{2,t}$ (in-phase solutions), right column: orbit diagrams of the carbon levels difference when $s_{1,t} \neq s_{2,t}$ (all other solutions), for different values of κ. The red areas in all the figures indicate the coexistence of in-phase and out-of-phase solutions for that parameter value.

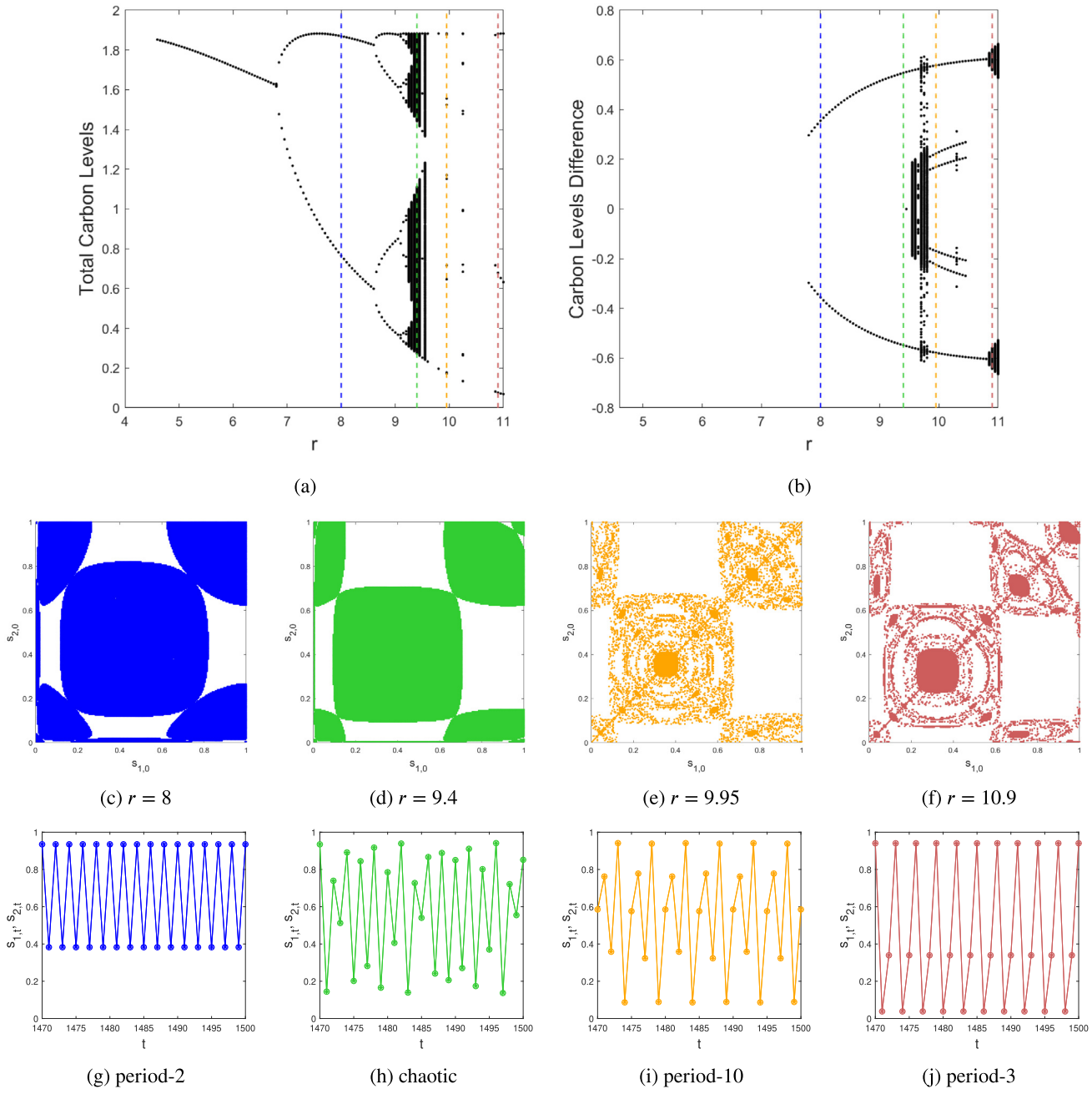

Fig. 8. (a) and (b) The orbit diagram of in-phase ($s_{1,t} = s_{2,t}$) and out-of-phase ($s_{1,t} \neq s_{2,t}$) solutions for $\kappa = 0.1$. (b)–(f) The basin of attraction for the in-phase solutions for different values of r and different patterns of oscillation (color coded to match the marker lines on (a) and (b)). (g)–(j) The corresponding pattern of in-phase oscillations for $s_{1,t}$, $s_{2,t}$, and $s_{1,t} + s_{2,t}$.

in Fig. 8 are in the form of period-2 oscillation for $r = 8$ (Fig. 8c and g), chaotic for $r = 9.4$ (Fig. 8d and h), period-10 for $r = 9.95$ (Fig. 8e and i), and period-3 when $r = 10.9$ (Fig. 8f and j). The general patterns of the basins of attraction are similar for different values of r (different patterns of in-phase solution), however, the density and the distribution of points differ, which can provide hints toward the prevalence of the attractor in the phase space. For example, the high density and the uniform distribution of points in Fig. 8c indicates that the period-2 attractor has a higher probability of emerging when $r = 8$ compared to the period-3 attractor (Fig. 8f) when $r = 10.9$ which has a nonuniform basin with lower density areas.

6. Discussion

We developed a new model for the alternate bearing phenomenon. Alternate bearing is defined as the variability of the production in many types of plants in a biennial manner. Similar to the Resource Budget Model, our new model is based on the balance between generating and storing nutrient during photosynthesis and other nutrient uptake processes and consuming it through flowering and nut production. We considered two biologically motivated criteria: 1) the limited capacity of each plant to store nutrient, and 2) low but non-vanishing yield during OFF-years (when the resource level is low). The limited capacity of the

resource tank was also considered in the generalized Resource Budget Model proposed by Ye and Sakai (2016). There are multiple mathematical functions that can satisfy the above conditions. In each case different constraints should be applied to keep the model biologically meaningful. Therefore, the model can be written in different mathematical forms while the qualitative dynamics of the model remains robust.

As it was observed in the experimental data in Ye et al. (2008), the return map of the fruit production shows a hump-shaped curve. Ye and Sakai reproduced this behavior by replacing the linear relationship between resource level and the cost of flowering and fruit production in the original Resource Budget Model with a Ricker-type function which introduced more parameters to the model (Ye and Sakai, 2016). We chose proper nonlinear functions, that satisfy the biologically motivated conditions mentioned above, to model the Nutrient Accumulation and Cost of Reproduction in our model. As a result the return map of the resource level and, consequently, the yield of the plant show a logistic-like curve. Therefore, unlike the Resource Budget Model, the new model for alternate bearing has stable period-2 solutions for a wide range of the model's parameters and is well suited to model the variable yield of plants in which the two-cycle behavior is more pronounced. The structure of our model makes it possible to nondimentionalize the resource level of the plant and, therefore, lower the number of parameters to three. Furthermore, by setting the nutrient accumulation efficiency and the reproductive investment rates to be equal, we further lower the number of parameters to two which makes the model easier to analyze and manipulate. However, the behavior of the model remains qualitatively the same if the two rates are not the same.

Trees in an orchard or natural forest do not show a perfect periodic reproduction since they are subject to environmental fluctuations. Although these variations affect the nutrient uptake and reproduction differently, they are not independent. To account for environmental stochasticity, we added two uncorrelated noise terms to the accumulation efficiency and the reproductive investment rates. Our analysis shows that adding stochasticity to the model affects the amplitude and phase of the oscillation of the tree's yield which models the noisy two cycle behavior observed in alternate bearing plants. To include the correlation between different environmental factors, one can use correlated noise terms. In this case, the correlation coefficient between the two noise terms becomes an additional parameter of the model.

Masting and spatial synchrony is observed among alternate bearing plants in orchards or natural forests. As the primary step to examine the behavior of our model on a collective level, we analyzed the dynamics of a coupled two-tree system. One of the mechanisms behind masting is the local interaction between neighboring trees. This interaction can be direct (root grafting), indirect (pollen coupling), or a mixture of both. Since in diecious plants, the female trees cannot interact through pollen coupling, we used direct coupling to model the local interaction. The numerical and stability analysis of the coupled Resource Budget Model with diffusive coupling showed that the only stable two cycle solution is the out-of-phase solution. Therefore, the Resource Budget Model cannot reproduce the spatial synchrony observed among female trees of the diecious plants for which root grating (direct coupling) is the main interaction mechanism. Our analysis shows that our new model for alternate bearing with direct coupling has stable in-phase period-2 solutions for a wide range of parameters and different values of coupling strength (κ). Having stable in-phase solutions can be interpreted as the primary requirement for the model to be used in studying spatial synchrony at a larger scale.

CRediT authorship contribution statement

Shadisadat Esmaeili: Methodology, Software, Formal analysis, Writing - original draft. **Alan Hastings:** Conceptualization, Methodology, Writing - review & editing. **Karen Abbott:** Conceptualization, Methodology, Writing - review & editing. **Jonathan Machta:** Conceptualization, Methodology, Writing - review & editing. **Vahini Reddy Nareddy:** Methodology, Writing - review & editing.

Declaration of Competing Interest

The authors declare that they have no known competing financial interests or personal relationships that could have appeared to influence the work reported in this paper.

Acknowledgement

We thank Patrick Brown and Todd Rosenstock for useful discussions. This work is supported by NSF grant DMS-1840221.

Appendix A. Stability Analysis of Period-2 Solutions in the Resource Budget Model

As it is shown in the orbit diagram of the Resource Budget Model in Fig. 1, RBM has one fixed point $\hat{s} = \frac{1}{1+m}$ which is stable for $m < 1$. The period-2 solution, if exists, is the fixed point of $s_{t+2} = f(s_t)$, where $f(s_t)$ can be obtained by iterating the model twice. Using Eq. (2) we will have,

$$s_{t+2} = f(s_t) = \begin{cases} s_t + 2, & s_t \leqslant -1 \\ -ms_t + (1-m), & -1 < s_t \leqslant 0 \\ m^2 s_t + (1-m), & 0 < s_t < \frac{1}{m} \\ -ms_t + 2. & s_t \geqslant \frac{1}{m} \end{cases} \tag{A.1}$$

Solving $s_{t+2} = s_t = \hat{s}$, we obtain three acceptable answers from the second, third, and fourth conditions in Eq. (A.1),

$$\hat{s} = \begin{cases} \frac{1-m}{1+m}, & -1 < \hat{s} \leqslant 0 \\ \frac{1}{1+m}, & 0 < \hat{s} < \frac{1}{m} \\ \frac{2}{1+m}. & \hat{s} \geqslant \frac{1}{m} \end{cases} \tag{A.2}$$

For $m > 1$ all solutions become unstable. On the other hand, if $m < 1$ the first and the third solutions become unacceptable since they do not satisfy their required conditions. The second solution is the model's stable fixed point and not a period-2 solution.

For $m = 1$ there is a continuum of period-2 solutions where the system oscillates between any values of $\hat{s}_1$ and $\hat{s}_2$, as long as $0 < (\hat{s}_1, \hat{s}_2) < 1$, and $\hat{s}_1 + \hat{s}_2 = 1$. To analyze the stability of these attractors, we study the system's response to small and large perturbations. Any small perturbation that keeps s_t between 0 and 1 will push the system into another period-2 attractor where the system will oscillate between two different values of $\hat{s}_1$ and $\hat{s}_2$. On the other hand, a large perturbation can result in s_t falling outside the $(0, 1)$ range. In that case, the system will come back and settle in one of the period-2 attractors inside the continuum.

Appendix B. Stability Analysis of the Coupled Resource Budget Model

When coupling two trees together, three scenarios can be considered:

I) Stable fixed point

If both trees maintain the same resource levels above the threshold, we can write the model as,

$$s_{1,t+1} = -(m+\kappa)s_{1,t} + 1 + \kappa s_{2,t}$$
$$s_{2,t+1} = -(m+\kappa)s_{2,t} + 1 + \kappa s_{1,t}. \quad \text{(B.1)}$$

Setting $s_{1,t+1} = s_{1,t}$ and $s_{2,t+1} = s_{2,t}$, the fixed point of the system is $\hat{s}_1 = \hat{s}_2 = \frac{1}{1+m}$. To perform the stability analysis, we find the eigenvalues of the coefficient matrix,

$$A = \begin{pmatrix} -(m+\kappa) & \kappa \\ \kappa & -(m+\kappa) \end{pmatrix}, \quad \text{(B.2)}$$

to be $\lambda_1 = -m$ and $\lambda_2 = -m - 2\kappa$. Therefore, the fixed point of the system is only stable if $(m + 2\kappa) < 1$.

II) Both trees oscillating between two positive values

In this case, the model is the same as Eq. (B.1). If the trees are in-phase with the same amplitude, $s_{1,t} = s_{2,t}$, there is no net flow of resources between the trees and the systems will be the same as two uncoupled trees. Since for an individual tree there is only a continuum of 2-period solutions when $m = 1$, the trees will stay in-phase only if they are started with equal resource levels and $m = 1$.

If $s_{1,t} \neq s_{2,t}$, the trees can be out of phase oscillating between two positive values. In this case, the following two conditions will be true,

$$s_{1,t+2} - s_{2,t+2} = s_{1,t} - s_{2,t}$$
$$s_{1,t+1} + s_{2,t+1} = s_{1,t} + s_{2,t}. \quad \text{(B.3)}$$

Iterating Eq. (B.1) twice, we can write,

$$s_{1,t+2} - s_{2,t+2} = (m = 2\kappa)^2 (s_{1,t} - s_{2,t}). \quad \text{(B.4)}$$

This means that the first condition in Eq. (B.3) is satisfied if $(m + 2\kappa) = 1$. As for the second condition, we will have,

$$s_{1,t} + s_{2,t} = \frac{2}{1+m}. \quad \text{(B.5)}$$

To find the period-2 solution, we assume that both trees oscillate out-of-phase between $\hat{s}_{low}$ and $\hat{s}_{high}$ (both positive). Substituting these values in Eqs. (B.1), we will have,

$$\hat{s}_{high} = -(m+\kappa)\hat{s}_{low} + 1 + \kappa \hat{s}_{high}$$
$$\hat{s}_{low} = -(m+\kappa)\hat{s}_{high} + 1 + \kappa \hat{s}_{low}. \quad \text{(B.6)}$$

Using the criterion $(m + 2\kappa) = 1$ obtained from the first condition in Eq. (B.3), we will have,

$$\hat{s}_{low} + \hat{s}_{high} = \frac{2}{1+m} \quad \text{(B.7)}$$

Therefore, any combination of $\hat{s}_{low}$ and $\hat{s}_{high}$ that satisfies Eq. (B.7) is the solution of the system.

III) Both trees oscillating between the same positive and negative values

In this case the model can be written as,

$$s_{1,t+1} = -(m+\kappa)s_{1,t} + 1 + \kappa s_{2,t} \quad s_{1,t} > 0$$
$$s_{2,t+1} = (1-\kappa)s_{2,t} + 1 + \kappa s_{1,t} \quad s_{2,t} \leqslant 0. \quad \text{(B.8)}$$

The second iteration will be,

$$s_{1,t+2} = (1-\kappa)s_{1,t+1} + 1 + \kappa s_{2,t+1} \quad s_{1t+1} \leqslant 0$$
$$s_{2,t+2} = -(m+\kappa)s_{2,t+1} + 1 + \kappa s_{1,t+1} \quad s_{2,t+1} > 0. \quad \text{(B.9)}$$

We define,

$$X_t^{(1)} = s_{1,t} + s_{2,t}$$
$$X_t^{(2)} = s_{1,t} - s_{2,t}. \quad \text{(B.10)}$$

According to the conditions described in Eq. (B.3), for the out-of-phase oscillation, we can write,

$$X_{t+1}^{(1)} = X_t^{(1)}$$
$$X_{t+2}^{(2)} = X_t^{(2)}. \quad \text{(B.11)}$$

Applying the first and second iteration of the model in Eqs. (B.11),

$$X_t^{(1)} = \frac{3-4\kappa-m}{(1+m)(1-k)}$$
$$X_t^{(2)} = \frac{1}{1-\kappa}. \quad \text{(B.12)}$$

From here, we can obtain $s_{1,t} = \frac{2}{1+m}$ and $s_{2,t} = \frac{1-(m+2\kappa)}{(1-\kappa)(1+m)}$. We began our discussion assuming that $s_{1,t} > 0$ and $s_{2,t} \leqslant 0$. Our final result for $s_{1,t}$ is in agreement with our initial assumption. But for $s_{2,t}$ to be less than or equal 0, $(m + 2\kappa)$ should be greater than or equal one $((m + 2\kappa) \geq 1)$.

To analyze the stability of this solution, we can analyze the stability of the fixed point of the following pair of equations,

$$s_{1,t+2} = f(s_{1,t}, s_{2,t})$$
$$s_{2,t+2} = g(s_{1,t}, s_{2,t}). \quad \text{(B.13)}$$

Using Eqs. (B.8) and (B.9), the coefficient matrix will be,

$$A = \begin{pmatrix} -m-\kappa+m\kappa+2\kappa^2 & 2\kappa(1-\kappa) \\ -2\kappa(m+\kappa) & -m-\kappa+m\kappa+2\kappa^2 \end{pmatrix}. \quad \text{(B.14)}$$

Matrix A has two eigenvalues, $\lambda_1 = (\kappa m - m - \kappa + 2\kappa^2) - 2\kappa[(\kappa+m)(\kappa-1)]^{(1/2)}$, and $\lambda_2 = (\kappa m - m - \kappa + 2\kappa^2) + 2\kappa[(\kappa+m)(\kappa-1)]^{(1/2)}$. Since $\kappa < 1, \lambda_1$ and λ_2 are complex conjugates. The period-2 solution is stable if $|\lambda| < 1$. This results in $m < 1$.

Appendix C. An alternate version of the model

As we mentioned before, there are multiple mathematical functions that satisfy the criteria discussed in Section 3. As an example, we can use the Beverton–Holt function to model the Nutrient Accumulation process. Therefore, the amount of nutrients added to the tree during year t can be written as,

$$\text{Nutrient Accumulation} = \frac{r_1 S_{max} S_t}{S_{max} + (r_1 - 1)S_t} - S_t \quad \text{(C.1)}$$

where $r_1 > 1$ is the nutrient accumulation rate and S_{max} is the maximum capacity of the tree to accumulate nutrients. We can nondi-

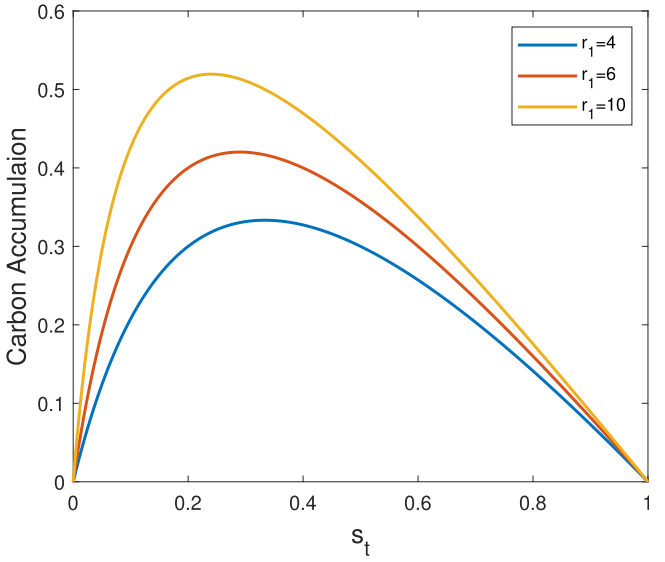

Fig. C.1. The behavior of the alternative Nutrient Accumulation function (Eq. (C.2)) for different values of efficiency rate.

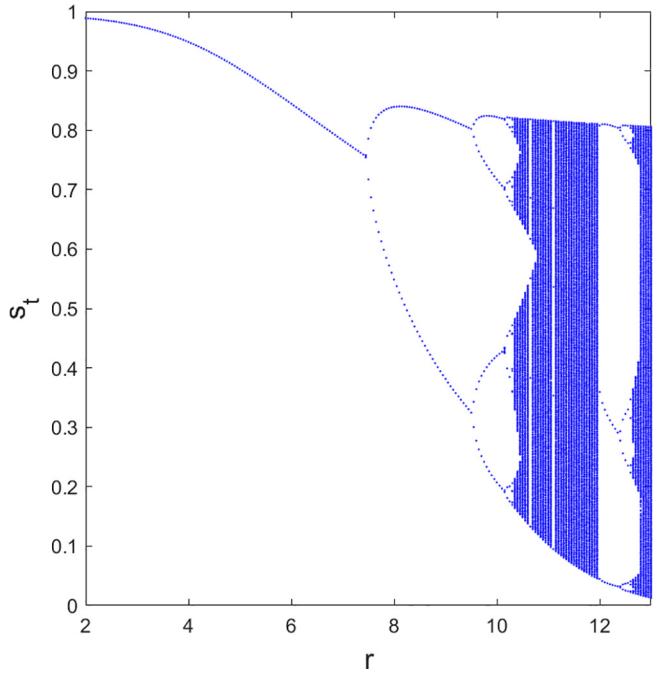

Fig. C.2. The orbit diagram of the alternate version of the model (Eq. (C.3)).

mensionalize Eq. (C.1) by defining $s_t = \frac{S_t}{S_{max}}$ and multiplying both sides by $\frac{1}{S_{max}}$. We will have,

$$\text{Nutrient Accumulation} = \frac{r_1 s_t}{1 + (r_1 - 1)s_t} - s_t. \tag{C.2}$$

Fig. C.1 shows the behavior of the Eq. (C.2) for different values of r_1.

We use the sigmoid function presented in Eq. (5) for the Cost of Reproduction. We can write the model as,

$$s_{t+1} = s_t + \left(\frac{r_1 s_t}{1 + (r_1 - 1)s_t} - s_t\right) - \left(\frac{1}{1 + e^{(-r_2 s_t + l)}} - \frac{1}{1 + e^{l}}\right). \tag{C.3}$$

As we can see in Fig. C.2, the orbit diagram of this version of the model is similar to the orbit diagram of the version proposed in the main text (Fig. 3a). This is an affirmation of the robustness of the model.

References

Devaney, R., 2003. An Introduction to Chaotic Dynamical Systems. CRC Press.

Feigenbaum, M.J., 1980. The metric universal properties of period doubling bifurcation and the spectrum for a route to turbulence. Ann. N.Y. Acad. Sci. 357 (1), 330–336.

Guignard, M.S., Leitch, A.R., Acquisti, C., Eizaguirre, C., Elser, J.J., Hessen, D.O., Jeyasingh, P.D., Neiman, M., Richardson, A.E., Soltis, P.S., Soltis, D.E., Stevens, C.J., Trimmer, M., Weider, L.J., Woodward, G., Leitch, I.J., 2017. Impacts of nitrogen and phosphorus: from genomes to natural ecosystems and agriculture. Front. Ecol. Evol. 5, 70.

Hastings, A., 1993. Complex interactions between between dispersal and dynamics: lessons from logistic equations. Ecology 74 (5), 1362–1372.

Isagi, Y., Sugimura, K., Sumida, A., Ito, H., 1997. How does masting happen and synchronize? J. Theor. Biol. 187, 231–239.

Klein, T., Siegwolf, R.T.W., Körner, C., 2016. Below ground carbon trade among tall trees in a temperate forest. Science 352 (6283), 342–344.

Lavee, S., 2007. Biennial bearing in olive (olea europaea). Ann. Ser. Hist. Nat. 17, 101–112.

Lyles, D., Rosenstock, T.S., Hastings, A., 2015. Plant reproduction and environmental noise: How do plants do it?. J. Theor. Biol. 371, 137–144.

Marino, G., La Mantia, M., Caruso, T., Marra, F.P., 2018. Seasonal dynamics of photosynthesis and total carbon gain in bearing and nonbearing pistachio (pistacia vera l.) shoots. Photosynthetica 56 (3), 932–941.

Marshall, B., Biscoe, P.V., 1980. A model for C_3 leaves describing the dependence of net photosynthesis on irradiance. J. Exp. Bot. 31 (120), 29–39.

Monselise, S.P., Goldschmidt, E.E., 1982. Alternate bearing in fruit trees. Horticul. Rev. 4, 128–173.

Noble, A.E., Rosenstock, T.S., Brown, P.H., Machta, J., Hastings, A., 2018. Spatial patterns of tree yield explained by endogenous forces through a correspondence between the ising model and ecology. PNAS 115 (8), 1825–1830.

Prasad, A., Sakai, K., 2015. Understanding the alternate bearing phenomenon: resource budget model. Chaos 25, 123102.

Prasad, A., Sakai, K., Hoshino, Y., 2017. Direct coupling: a possible strategy to control fruit production in alternate bearing. Sci. Rep. 7 (39890), 1–11.

Satake, A., Iwasa, Y., 2000. Pollen-coupling of forest trees: forming synchronized and periodic reproduction out of chaos. J. Theor. Biol. 203, 63–84.

Shalom, L., Samuels, S., Zur, N., Shlizerman, L., Zemach, H., Weissberg, R.O., Blumwald, E., Sadka, A., 2012. Alternate bearing in citrus: changes in the expression of flowering control genes and in global gene expression in on-versus off-crop trees. PLoS One 7, (10) e46930.

Strogatz, S., 1994. Nonlinear Dynamics and Chaos: With Applications to Physics, Biology, Chemistry, and Engineering. West View Press, Reading, MA.

Ye, X., Sakai, K., 2016. A new modified resource budget model for nonlinear dynamics in citrus production. Chaos Solitons Fract 87, 51–60.

Ye, X., Sakai, K., Asada, S., Sasao, A., 2008. Inter-relationship between canopy features and fruit yield in citrus as detected by airborne multispectral imagery. Trans. ASABE 51, 739–751.